AGU PUBLICATIONS

JGR

Journal of Geophysical Research: Atmospheres

RESEARCH ARTICLE
10.1002/2017JD027111

Key Points:
- The mass accommodation coefficients should be greater than 0.4, 0.2, and 0.4 for EG, DEG, and 1-butanol, respectively
- The relative standard deviation of the calculated diffusion constant for glycerol is improved from ±8% to between −3% and 1%

Correspondence to:
J. P. Reid,
j.p.reid@bristol.ac.uk

Citation:
Su, Y.-Y., Marsh, A., Haddrell, A. E., Li, Z.-M., & Reid, J. P. (2017). Evaporation kinetics of polyol droplets: Determination of evaporation coefficients and diffusion constants. *Journal of Geophysical Research: Atmospheres*, *122*, 12,317–12,334. https://doi.org/10.1002/2017JD027111

Received 10 MAY 2017
Accepted 22 OCT 2017
Accepted article online 26 OCT 2017
Published online 22 NOV 2017

Evaporation Kinetics of Polyol Droplets: Determination of Evaporation Coefficients and Diffusion Constants

Yong-Yang Su[1], Aleksandra Marsh[2], Allen E. Haddrell[2], Zhi-Ming Li[1], and Jonathan P. Reid[2]

[1]Northwest Institute of Nuclear Technology, Xi'an, China, [2]School of Chemistry, University of Bristol, Bristol, UK

Abstract In order to quantify the kinetics of mass transfer between the gas and condensed phases in aerosol, physicochemical properties of the gas and condensed phases and kinetic parameters (mass/thermal accommodation coefficients) are crucial for estimating mass fluxes over a wide size range from the free molecule to continuum regimes. In this study, we report measurements of the evaporation kinetics of droplets of 1-butanol, ethylene glycol (EG), diethylene glycol (DEG), and glycerol under well-controlled conditions (gas flow rates and temperature) using the previously developed cylindrical electrode electrodynamic balance technique. Measurements are compared with a model that captures the heat and mass transfer occurring at the evaporating droplet surface. The aim of these measurements is to clarify the discrepancy in the reported values of mass accommodation coefficient (α_M, equals to evaporation coefficient based on microscopic reversibility) for 1-butanol, EG, and DEG and improve the accuracy of the value of the diffusion coefficient for glycerol in gaseous nitrogen. The uncertainties in the thermophysical and experimental parameters are carefully assessed, the literature values of the vapor pressures of these components are evaluated, and the plausible ranges of the evaporation coefficients for 1-butanol, EG, and DEG as well as uncertainty in diffusion coefficient for glycerol are reported. Results show that α_M should be greater than 0.4, 0.2, and 0.4 for EG, DEG, and 1-butanol, respectively. The refined values are helpful for accurate prediction of the evaporation/condensation rates.

1. Introduction

Understanding and quantifying the kinetics of mass transfer between the gas and condensed phases in aerosol is important for predicting mass concentrations, size distributions, and compositions with consequences for ambient aerosol processes, impacts, and fates (Riipinen et al., 2011, 2012; Topping et al., 2013; Tröstl et al., 2016). Predictions of condensation and evaporation rates depend on accurate knowledge of physicochemical properties of the gas and condensed phases, such as vapor pressures, diffusion constants, and thermal conductivities (Miles et al., 2012), and kinetic parameters such as mass/thermal accommodation coefficients, which are crucial for estimating mass fluxes over a wide size range extending from the free molecule to continuum regimes (Kolb et al., 2010; Vehkamäki & Riipinen, 2012). These quantities are generally much less well known for condensing and evaporating organic vapors than for water (Kolb et al., 2010). In addition, many of these same quantities and processes must be accurately represented in the design and interpretation of data from analytical instruments such as the condensation particle counter (CPC) and the hygroscopic tandem differential mobility analyzer.

The CPC is the most commonly used technique for ultrafine-particle concentration measurements in laboratory and field measurements (McMurry, 2000). Inside the CPC, a gas phase supersaturation of a condensing species is generated through which the introduced particles are activated and grow to sizes that are large enough for optical detection. Various types of laminar, continuous flow CPCs have been developed as commercial instruments using different working fluids, e.g., 1-butanol (Agarwal & Sem, 1980), water (Hering & Stolzenburg, 2005), and diethylene glycol (Iida et al., 2009). Iida et al. (2009) investigated the dependence of the size-dependent activation efficiency on the working fluid, considering ethylene glycol, diethylene glycol, propylene glycol, oleic acid, and dioctyl sebacate. Diethylene glycol (DEG) was recommended as the most effective working fluid in new CPC designs, improving the performance of sub-2 nm particle detection. Furthermore, several CPC-based techniques, such as Pulse Height Analysis Mode (Saros et al., 1996), the CPC battery (Kulmala et al., 2007), and the Nano-CPC battery (Kangasluoma et al., 2014), have been proposed to obtain more information in atmospheric nanoparticles measurement other than just the particle concentration. The calibration and application of different types of CPC show that the

detection efficiency is dependent not only on the instrumental operating conditions (pressure, flow rate, and temperature) but also on the particle properties (initial size, polarity, chemical composition, and morphology) (Giechaskiel et al., 2011; Hering & Stolzenburg, 2005; Kangasluoma et al., 2015; Kulmala et al., 2007; Tuch et al., 2016; Wiedensohlet et al., 1997; Zhang & Liu, 1990). Therefore, numerical simulations of condensational growth of particles inside the CPC are essential for instrument development and data interpretation (Ahn & Liu, 1990; Hering & Stolzenburg, 2005; Iida et al., 2009; Saros et al., 1996; Zhang & Liu, 1990).

The supersaturation profile of the working fluid vapor inside the condenser of a CPC is calculated from the vapor species and temperature distributions, both of which are calculated from flow field simulations. Equations satisfying heat balance have been developed to describe the particle growth process (Ahn & Liu, 1990; Zhang & Liu, 1990). Transition regime corrections are taken into account (Seinfeld & Pandis, 2006) to ensure that the equations are valid for the entire particle size range sampled. In the free molecule regime, mass accommodation coefficient (α_M) and thermal accommodation coefficient (α_T) are the two parameters that fundamentally influence the interaction of the vapor with growing droplets (Seinfeld & Pandis, 2006; Winkler et al., 2004). A value of $\alpha_M < 1$ has the implication that the actual final size of a droplet is smaller than the predicted value when assuming that $\alpha_M = 1$. Kinetic calculations show that the time dependence of water droplet growth is more sensitive to α_M than α_T (Miles et al., 2012) for particle sizes in the CPC measurement size range. Therefore, α_M is a key parameter that must be known to fully understand and quantify the condensational growth of particles. The mass accommodation coefficient (α_M) and evaporation coefficient (γ) are referred to in condensation and evaporation studies, respectively. However, the values of α_M and γ are assumed to be identical based on microscopic reversibility (Miles et al., 2012).

For water, many studies have reported α_M through measurements of evaporation/condensation kinetics (Davies et al., 2014; Hołyst et al., 2013; Langridge et al., 2016; Marek & Straub, 2001; Miles et al., 2012; Raatikainen et al., 2012; Tsuruta et al., 1994; Winkler et al., 2006). Results from experiments using a variety of ensemble and single-particle techniques confirm that α_M is greater than 0.2 (Langridge et al., 2016; Miles et al., 2012) and even close to 1 (Davies et al., 2014; Raatikainen et al., 2012; Winkler et al., 2006). α_T is usually assumed to be unity, which agrees with simulation and experimental results (Hołyst et al., 2013; Winkler et al., 2004; Zientara et al., 2008). The temperature dependence of the vapor pressure of water (Davies et al., 2014; Murphy & Koop, 2005) and the diffusion coefficient of water in the gas phase are well established (Miles et al., 2012). In this work, further measurements of the evaporation kinetics of pure water are only reported to verify model performance.

For 1-butanol, Ahn and Liu (1990) assumed $\alpha_M = 1$ in their simulations of condensational growth inside a 1-butanol CPC. However, this assumption cannot be verified based on current design because the droplet size as a function of time could not be adequately resolved. Very few studies to determine α_M for 1-butanol have been reported. Only the product of diffusion coefficient and vapor pressure ($D \times p_v$), which is a constant under quasi-steady state conditions (Fuchs, 1959), was determined by Erbil and Dogan (2000) for some liquids from hanging droplet evaporation measurements, including 1-butanol. Taking into account the temperature suppression at the droplet surface but not α_M, the reported value of $D \times p_v$ for 1-butanol at 14.9°C was 0.435 $cm^2\ s^{-1}$ mmHg. This value is 52% higher than the product of D and p_v both at 14.9°C presented in the same paper, which suggests that there is a large error in the determined value of $D \times p_v$.

Tsuruta et al. (1994) determined the α_M of ethylene glycol (EG) and water using a dropwise condensation method. They reported that the α_M value for EG is in the range of 0.17–0.45 at 0.24–1.57 kPa. Jakubczyk et al. (2010) investigated the evaporation kinetics of some low-volatility organic (EG, DEG, and TEG) droplets in nitrogen. Their results suggested that the evaporation coefficient for EG at 298 K is as low as 0.035 ± 0.012.

The evaporation rates of DEG, TEG, and glycerol into vacuum have been measured in the temperature range 5–50°C using a microbalance (McFeely & Somorja, 1972). Results suggested that the value of evaporation coefficient for DEG at 300 K is 0.05. Lednovich and Fenn (1977) measured the absolute evaporation flux of some polar and nonpolar liquids (including DEG and glycerol) from clean surface by means of a mass spectrometer. The values of evaporation coefficient were reported to be close to unity (0.98–1.2 for DEG at

4.5–37.3°C) and independent of temperature. However, the value determined in later experimental work was only 0.082 ± 0.035 for DEG at 298 K (Jakubczyk et al., 2010). Recently, Hołyst et al. (2013) used molecular dynamics simulation and single-particle technique to investigate the interfacial transport of energy and mass during evaporation of liquid droplets of water, DEG, TEG, and glycerol into inert gas. They found that α_M for DEG lies within the range of 0.74–0.9.

For glycerol, the experimentally determined values of α_M are as follows: 0.34 at 300 K (McFeely & Somorja, 1972), 0.89–0.98 in the temperature range of 19.1–62.1°C (Lednovich & Fenn, 1977), and 1 in the temperature range of 291–341 K (Cammenga, Schulze, & Theuerl, 1977). The diffusion coefficient of glycerol is not included in the commonly used handbooks (Dean, 1999; Haynes, 2016) or compilations (Lugg, 1968; Tang et al., 2015a). Instead, the value used in previous study (Davies, 2014) is estimated from kinetic theory and has an estimated uncertainty of ±8% (Bird et al., 2002).

In this study, we aim to clarify the discrepancy in α_M values for 1-butanol, EG, and DEG and improve the accuracy of D for glycerol. The order of volatility of decreasing volatility is 1-butanol, EG, DEG, and glycerol. We will use a model based on the work of Ahn and Liu (1990) (referred to as the Liu model below) to describe the heat and mass transfer at the evaporating droplet surface. In order to verify a newly developed program based on the Liu model, the evaporation kinetics of pure water droplets under different relative humidities (RHs) are simulated and compared with cylindrical electrode electrodynamic balance (EDB) measurements and with a further model that we have used previously (Miles et al., 2012). The sensitivity of the evaporation kinetics of 1-butanol to the value of α_M is also analyzed. Then, we will report the evaporation profiles of 1-butanol, EG, DEG, and glycerol droplets under well-defined conditions (gas flow rates and temperature) using the previously developed EDB technique (Davies et al., 2013, 2014, 2012; Rovelli et al., 2016). For single-component organic droplets, the time-resolved radius recorded from experiments is fit using Liu model with varying experimental conditions (e.g., gas velocity, V_g) and differing treatments of the key thermophysical properties (specifically, the evaporation coefficient, α_M, and the relative error in the literature value of diffusion coefficient at 298 K, $\Delta D_{298}/D_{298}$). The fitted values of (α_M, V_g, and $\Delta D_{298}/D_{298}$) corresponding to the best agreement between model prediction and experimental data (minimum residual) are obtained. With knowledge of uncertainties in the thermophysical and experimental parameters, the plausible ranges of the evaporation coefficients for 1-butanol, EG, and DEG as well as uncertainty in D for glycerol are reported.

2. Modeling Evaporation Kinetics of a Single-Component Droplet

2.1. Evaporation/Condensation Model

Models for predicting evaporation/condensation rates of unary, binary, and more complex droplets have been developed by a number of authors (Jakubczyk et al., 2010; Kulmala et al., 1993; Persad & Ward, 2016; Seinfeld & Pandis, 2006). If the temperature suppression at the evaporating droplet surface is severe (i.e., the temperature difference between the droplet surface and the surrounding gas, $T_d - T_\infty$, is greater than −3 K), the semianalytical framework of Kulmala et al. (1993) is not accurate (Kulmala et al., 1993; Rovelli et al., 2016). Considering the simplicity of the treatment for a single-component droplet while capturing the possible coupling of heat and mass transport, the Liu model (Ahn & Liu, 1990) is compared with our measurements. The radius (r) of the evaporating/condensing single-component droplet as a function of time (t) can be described as

$$r\frac{\mathrm{d}r}{\mathrm{d}t} = \frac{DM_v}{\rho R}\left(\frac{p_\infty}{T_\infty} - \frac{p_d}{T_d}\right)\beta_M \tag{1}$$

$$T_d - T_\infty = \frac{LDM_v}{K_g R}\left(\frac{p_\infty}{T_\infty} - \frac{p_d}{T_d}\right)\frac{\beta_M}{\beta_T} \tag{2}$$

where D is the diffusion coefficient of the evaporating/condensing vapor in the surrounding gas (pure nitrogen in this work). M_v and ρ are the vapor's molar mass and liquid phase density, respectively. R is the gas constant. p_d and p_∞ are the partial pressures of the evaporating/condensing vapor at the droplet surface and far from the surface, respectively, and T_d and T_∞ are the corresponding temperatures. K_g is the thermal conductivity of the surrounding gas, and L is the latent heat (enthalpy of vaporization) of the evaporating/condensing vapor. β_M and β_T are the Fuchs-Sutugin transitional correction factors for mass

and heat transfer, respectively. β_M and β_T are expressed as (Kulmala et al., 1993; Miles et al., 2012; Seinfeld & Pandis, 2006; Winkler et al., 2004)

$$\beta_M = \frac{1 + Kn_M}{1 + \left(\frac{4}{3\alpha_M} + 0.377\right)Kn_M + \frac{4}{3\alpha_M}Kn_M^2} \tag{3}$$

$$\beta_T = \frac{1 + Kn_T}{1 + \left(\frac{4}{3\alpha_T} + 0.377\right)Kn_T + \frac{4}{3\alpha_T}Kn_T^2} \tag{4}$$

$$Kn_M = \frac{\lambda_M}{r} \tag{5}$$

$$Kn_T = \frac{\lambda_T}{r} \tag{6}$$

Kn_M and Kn_T are the Knudsen number for mass and heat transfer, respectively (Ahn & Liu, 1990; Wagner, 1982). λ_M and λ_T are the effective mean free paths for mass and heat transfer, respectively (Seinfeld & Pandis, 2006).

$$\lambda_M = \frac{3D}{\overline{c_v}} \tag{7}$$

$$\overline{c_v} = \left[\frac{8k_BT}{\pi m_v}\right]^{1/2} = \left[\frac{8RT}{\pi M_v}\right]^{1/2} \tag{8}$$

$$\lambda_T = \frac{3D}{\overline{c_g}} \tag{9}$$

$$\overline{c_g} = \left[\frac{8RT}{\pi M_g}\right]^{1/2} \tag{10}$$

$\overline{c_v}$ and $\overline{c_g}$ are the mean speeds of vapor and gas molecules at temperature of T, respectively. M_g is the molar mass of the surrounding gas.

Finally,

$$p_\infty = S{\cdot}p_v(T_\infty) \tag{11}$$

$$p_d = a_{\text{solute}}{\cdot}a_{\text{Kelvin}}{\cdot}p_v(T_d) \tag{12}$$

where S is the saturation fraction of vapor in the flowing gas far from the droplet surface, a_{solute} and a_{Kelvin} are correction factors taking into account the solute effect and Kelvin effect, respectively, and $p_v(T_\infty)$ and $p_v(T_d)$ are vapor pressures of the evaporating vapor at T_∞ and T_d, respectively (Seinfeld & Pandis, 2006).

2.1.1. Modifications and Corrections

The mass flux of a pure (single-component) droplet during evaporation/condensation is defined by

$$I = \frac{dm}{dt} = 4\pi\rho r^2\frac{dr}{dt} \tag{13}$$

When both sides of equation (1) are multiplied by r, the left side is proportional to the mass flux, I, as shown in equation (13). Taking into account the enhanced mass transfer due to the relative movement of the droplet and gas phase, the right sides of equations (1) and (2) are scaled as

$$r\frac{dr}{dt} = \frac{Sh}{2}\frac{DM_v}{\rho R}\left(\frac{p_\infty}{T_\infty} - \frac{p_d}{T_d}\right)\beta_M \tag{14}$$

$$T_d - T_\infty = \frac{Sh}{2}\frac{LM_vD}{K_gR}\left(\frac{p_\infty}{T_\infty} - \frac{p_d}{T_d}\right)\frac{\beta_M}{\beta_T} \tag{15}$$

The Sherwood number, Sh, is defined as a function of other dimensionless parameters (Seinfeld & Pandis, 2006)

$$Sh = 2 + 0.6\,\text{Re}^{1/2}Sc^{1/3} \tag{16}$$

$$\text{Re} = \frac{2rV_g}{\upsilon_g} \tag{17}$$

$$Sc = \frac{\upsilon_g}{D} \tag{18}$$

Table 1
Physicochemical Properties of 1-Butanol, EG, DEG, and Glycerol From Literatures and the Concentrations of the Prepared Solutions

Compounds	1-butanol	EG	DEG	Glycerol
ρ /Kg m^{-3}	$\rho(T)=\rho_c\left[1+\sum_{i=1}^{N_p} a_i(1-T_r)^{i/3}\right]$, $T_r=T/T_c$ P_c = 271.00 kg m^{-3}, $a_1=-3.57379$, $a_2=5.02450\cdot10$, $a_3=-1.75934\times10^2$, $a_4=3.08588\times10^2$, $a_5=-2.65628\times10^2$, $a_6=8.94997\times10$, T_c = 563.01 K, (Haynes, 2016)	1113.5–293.15 K	1120–293.15 K	1261.3–293.15 K
p_v/Pa	$\log_{10}(P_v/133.322)=39.6673-4.0017\times10^3/T-10.295\times\log_{10}(T)-3.2572\times10^{-10}T+8.6672\times10^{-7}T^2$, (Yaws, 1994)	$\ln(P_v)=84.09-\frac{10411}{T}-8.1976\times\ln(T)+1.6536\times10^{-18}T^6$, T: K, Range: 260.15–720 K, (Ethylene Glycol Product Guide, 2008)	$\ln(P_v)=116.21594-\frac{13273.461}{T}-12.665825\times\ln(T)+5.9330303\times10^{-29}T^{10}$, T: K, Range: 283–523 K, (DiEthylene Glycol Product Guide, 2005)	$\log_{10}(P_v/133.322)=41.98405-\frac{6024.479}{T}-10.3272\times\log_{10}(T)$, (Cammenga et al., 1977)
D_{298}/m^2 s^{-1}	8.61×10^{-6} (RSD = 1.1%), (Lugg, 1968)	1.01×10^{-5} (RSD = 3.8%), (Lugg, 1968)	7.30×10^{-6} (RSD = 1.0%), (Lugg, 1968)	7.63×10^{-6} (Estimated Using Chapman-Enksog Theory, Bird et al., 2002)
L/kJ mol^{-1}	$L=C_1(1-T_r)^{C_2+C_3T_r+C_4T_r^2+C_5T_r^3}$, $T_r=T/T_c$ $C_1=7.1274\times10^7$, $C_2=0.0483$, $C_3=0.8966$, $C_4=-0.5116$, $C_5=0$, T_c = 563.01 K, (Poling et al., 2008)	63.9–298 K (Haynes, 2016)	66.64–298 K (https://pubchem.ncbi.nlm.nih.gov)	61.66–298 K (https://pubchem.ncbi.nlm.nih.gov)
Solute concentration/g L^{-1} (solvent)	687.3 (Ethanol/H_2O = 1:1 *v/v*)	604.4 (H_2O)	530.1 (H_2O)	493.5 (H_2O)

where Re is the Reynolds number, V_g is the gas flow velocity, v_g is kinematic viscosity of gas, and Sc is the Schmidt number. This correction is the same as used by previous researchers (Davies et al., 2012; Devarakonda & Ray, 2000; Hopkins & Reid, 2005).

2.1.2. Properties of Nitrogen and Organic Vapor

The thermal conductivity (K_g) and kinematic viscosity (v_g) for nitrogen have been well characterized, and the parameterizations are given by Lemmon and Jacobsen (2004). By fitting the data from these parameterizations, simpler forms are obtained for easy use (Davies, 2014) and will be used in this work as $K_g=3.95\times10^{-4}+9.805\times10^{-5}T-4.3032\times10^{-8}T^2$, and $v_g=8.263\times10^{-8}T-8.722\times10^{-6}$. The main physicochemical properties of compounds investigated in this work are listed in Table 1. For 1-butanol, although many parameterizations of vapor pressure (p_v) have been presented, the relative differences among the calculated values are several percent or even higher. The parameterization of p_v from Yaws (1994) was used for simulation in this work because the predicted value at 298 K (940 Pa) matches the most recent experimental value (Garriga et al., 2002).

The temperature dependence of D is described as (Tang et al., 2015a)

$$D=D_{298}\left(\frac{T}{298}\right)^{1.75} \tag{19}$$

where D_{298} is the diffusion coefficient at 298 K, as shown in Table 1.

Under the conditions investigated ($S\approx0$), the temperature difference (T_d-T_∞) for an evaporating 1-butanol droplet is ~−3 K, while the (T_d-T_∞) values are smaller than −0.075, -3×10^{-3}, and -2×10^{-4} K for evaporating EG, DEG, and glycerol droplets, respectively. For 1-butanol, the temperature dependences of density and latent heat were taken into account, and the parameterizations from Haynes (2016) and Poling et al. (2008), respectively, were used in this study, as shown in Table 1. The densities for EG, DEG, and glycerol at 20°C (Haynes, 2016) were used throughout in the simulation. As their latent heat is insensitive to temperature in the range of interest (15–25°C), the values at 25°C from database (Haynes, 2016, https://pubchem.ncbi.nlm.nih.gov) are used directly in the simulation.

2.2. Verification of the Fitting Procedure Based On the Liu Model

A program based on the Liu model was written in MATLAB® and then verified by comparing predictions for evaporation of pure water droplets with experimental results. Another well-developed program which is

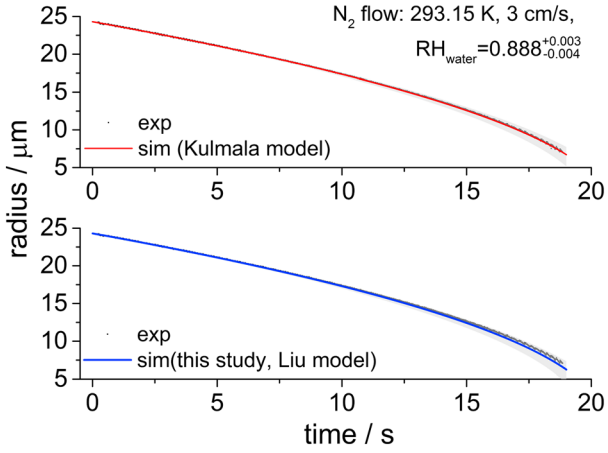

Figure 1. Evaporation profiles of pure water droplet into humid nitrogen flow: Experimental versus model predictions.

based on Kulmala semianalytical model (Davies et al., 2012; Miles et al., 2012) was used as a benchmark for comparison.

Comparative kinetic measurement for hygroscopicity determination of aerosol using the EDB has been described previously (Davies et al., 2013; Rovelli et al., 2016). Similarly, we use the size of an equilibrated sodium chloride droplet to determine the RH in the gas phase and measure the evaporation kinetics of a pure water droplet into a gas phase of varying RH for comparison. The sodium chloride droplet, starting with known initial solute concentration, and a pure water droplet were sequentially generated and introduced into the chamber as probe and sample droplets, respectively. The equilibrated size following evaporation of the aqueous NaCl droplet can be used to determine the gas phase RH (Davies et al., 2013; Rovelli et al., 2016). For example, in Figure 1, the gas phase RH determined using NaCl probe is $0.888^{+0.003}_{-0.004}$. Then, the evaporation profile of a pure water at RH = 0.888 is predicted using Kulmala and Liu models, as shown in Figure 1. The simulated evaporation profile using the Kulmala model agrees well with the experimental results. Although the Liu model used in this study slightly overestimates the evaporation rate, the simulated curve still matches the experimental curve within the uncertainty envelope. The expressions of the Liu model are simple and explicit, and it is for this reason that the Liu model is used throughout in the work. The comparison in Figure 1 serves as a validation of our implementation of the Liu model, clearly demonstrating that it is sufficiently accurate to describe the evaporation/condensation kinetics of compounds investigated in this work.

2.3. Sensitivity of Evaporation Kinetics on α_M

Figure 2 shows simulated evaporation profiles of a pure 1-butanol droplet assuming $T = 293.15$ K, $V_g = 3$ cm/s, and $S = 0$ in the nitrogen flow. The sensitivity of evaporation kinetics of a pure 1-butanol droplet to mass accommodation coefficient (α_M) is illustrated by varying α_M = 0.1, 0.2, 0.4, 0.6, and 1 in calculations using the Liu model. As shown in Figure 2, the evaporation rate increases with α_M. Limited by the size accuracy in present EDB measurement (±100 nm) (Davies, 2014, Rovelli et al., 2016), it would not be possible to resolve the difference between α_M = 0.6 and 1 experimentally, as the error envelopes overlap.

By using equations (5), (7), and (8), the effective mean free path for mass transfer is estimated to be ~90 nm under the conditions investigated, which is 2 orders of magnitude smaller than the droplet radius recorded by the EDB (9–30 μm) in this study. Thus, the evaporation kinetics of organics investigated in this study are always in the continuum regime with values of $Kn < 0.01$. As the evaporation rates of EG, DEG, and glycerol are several orders of magnitude lower than that of 1-butanol, their evaporation kinetics are less sensitive to α_M. In the following model predictions for EG, DEG, and glycerol, α_M is also varied at 0.1, 0.2, 0.4, 0.6, and 1 to resolve its influence. However, only the results at α_M = 0.1, 0.2, 0.4, and 1 are presented and discussed.

3. Experimental

3.1. Reagents

For EG (>99%, Acros Organics), DEG (>99%, Alfa Aesar), and glycerol (>99.5%, Acros Organics) solutions, high-performance liquid chromatographygrade water (VWR Chemicals) was used. Solutions were prepared up to the solubility limit of each solute considered. For 1-butanol (>99%, Fisher) solution, an ethanol-H_2O mixture with volume ratio of unity (v/v = 1) was used as the solvent as 1-butanol is insoluble in water but miscible in ethanol. The solute concentrations of the solutions prepared in this study are listed in Table 1.

3.2. Time-Resolved Evaporation Profiles of Single Droplets

The EDB measurement procedures used in this study have been discussed in previous works (Davies et al., 2012, 2013; Rovelli et al., 2016). The electrodynamic potential is provided by a pair of concentric cylindrical

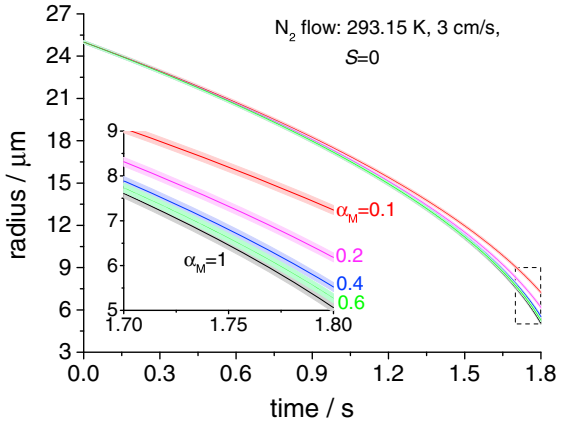

Figure 2. Simulated evaporation kinetics of pure 1-butanol droplet using different values of mass accommodation coefficient (α_M).

electrodes, and the trap is operated at atmospheric pressure and can access a temperature range from 248 to 340 K. A gas flow passes through the cylindrical electrodes, and the environmental conditions (flow rates, relative humidity, and temperature) are known and well controlled. More specifically, a dry or humidified nitrogen flow controlled by mass flow controller (MKS 1179A) is introduced into the chamber through the space between the inner electrode and the outer electrode. The temperature of the chamber body is controlled with high precision by a recirculating water/EG mixture (v/v = 1) from a thermostatic water bath (Julabo, F32). Single droplets generated on demand by a microdispenser (Microfab MJ-ABP-01) are charged using an induction electrode then introduced into the chamber and finally trapped in the central region between the electrodes within 100 ms. After careful collimation, the trapped droplet is illuminated by a green laser (λ = 532 nm). The elastic scattering pattern is recorded with high time resolution down to 10 ms. The levitated droplets remain spherical during measurement because the droplets are sufficiently small enough that capillary forces dominate the gravitational force (Reid et al., 2011). The Geometric Optics Approximation (GOA) method is used to calculate the droplet radius as time evolves (Davies et al., 2012).

In this work, full evaporation profiles of EG/water, DEG/water, and glycerol/water droplets (referred to as EG, DEG, and glycerol droplets later) at 20°C and under different flow rates (50, 100, and 200 cm^3/min) were recorded with a time resolution of 10 ms, as shown in Figures 3a–3c. Because of the high volatility of 1-butanol, evaporation profiles of 1-butanol/ethanol/water (referred to as a 1-butanol droplet) droplet at lower temperatures (12 and 15°C) were also recorded to collect more data for fitting, as shown in Figure 3d. The reported values of refractive index at 589 nm were used in the GOA method, as they are very close to

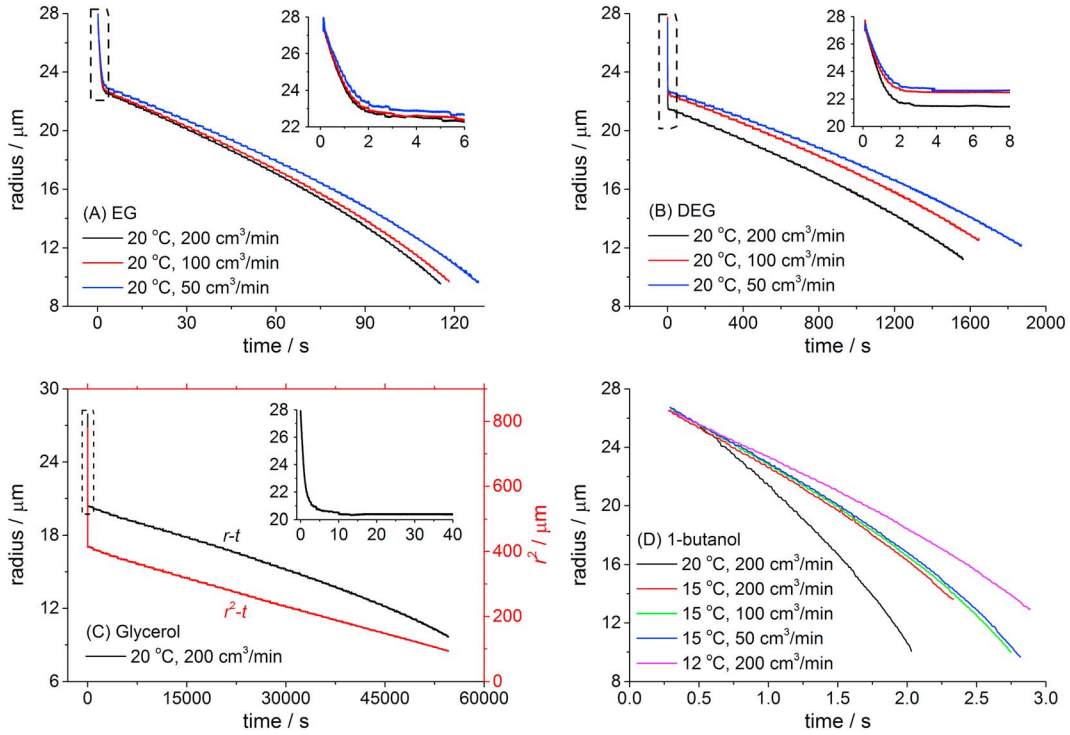

Figure 3. Evaporation profiles of (a)EG, (b) DEG, (c) glycerol, and (d) 1-butanol droplets in a pure dry nitrogen flow. Only one evaporation measurement for each aqueous-organic droplet is shown. The solution concentration and solvents are listed in Table 1.

those at 532 nm and can easily be found in the Haynes (2016). Repeated measurements were performed for ten 1-butanol droplets, three EG droplets, two DEG droplets, and two glycerol droplets for each set of environmental conditions.

For EG, DEG, and glycerol droplets evaporating in a pure dry nitrogen flow, the solvent (water) evaporates at least 2 orders of magnitude faster than that of the solute because of the high values of p_v and D for water. An inflection point in the r-t curve is easily observed (Figures 3a–3c) at around 2 s when water evaporation is nearly complete, and the evaporation kinetics become dominated by the low-volatility solute (Krieger et al., 2012). Therefore, only data beyond 30 s are considered for fitting to avoid the interference of solvent (water) evaporation and temperature suppression.

In the case of a 1-butanol droplet, the evaporation rates of cosolvents (ethanol: H_2O) are several times higher than that of 1-butanol although some residual water or ethanol might still remain in the droplet. As shown in Figure 3d, the inflection point in the r-t curve is not significant. Although the solute concentration is very high and the value is close to the density of pure 1-butanol (810 g/L), it is difficult to determine exactly when the mole fractions of ethanol/water become very small. Assuming that the solvents evaporate completely while 1-butanol remains in the droplet, the corresponding radius should be ~25 μm, a size which is reached at ~0.5 s. In the fitting procedures, data points beyond 0.8, 1.0, and 1.5 s (total evaporation time of around 2.5 s at 15°C) were used for fitting, respectively. The effect of the selected data range on the fitting results will be discussed later. The systematic influences of the gas velocity and temperature on the evaporation rates are clear in these plots, and the small variation with gas flow rate seen in Figure 3d illustrates the high level of precision that can be achieved using this approach.

3.3. Fitting of Experimental Data

As no organic vapors were introduced in the nitrogen flow during measurements, the saturation fraction, S, in equation (11) was set to be zero in the simulation. The correction factor for the solute effect (a_{solute}) equals unity for a single-component droplet. The possible effect of impurities introduced from reagents will be discussed later. For particles larger than 5 μm, the lower limit of experimental measurements in the current study, the correction factor for the Kelvin effect (a_{Kelvin}) is within the range of 1–1.0008 according to the equation in Hinds (1999). Thus, a_{Kelvin} is set to be unity in all cases. We now present the procedure used to fit the raw evaporation data for single-component droplet.

In a first preprocessing stage, the curves for radius and radius squared as a function of time (r-t and r^2-t) are considered. A linear regression method is used to obtain the best linear fit of the experimental r^2-t curve and to remove any outliers in radius. From this fit, the first fitted value of the square of radius ($r^2_{0,\text{fit}}$) and its uncertainty range (the lower limit, J_1, and the upper limit, J_2, in $r^2_{0,\text{fit}}$) are identified. In the following simulation, the trial value of r_0 is scanned in the range of ${J_1}^{1/2}$–${J_2}^{1/2}$ to account for this possible error in the initial droplet size determination (typically ±100 nm (Davies, 2014; Rovelli et al., 2016)).

For chosen values of mass accommodation coefficient (α_M) and gas flow velocity (V_g), the droplet temperature at its surface (T_d) is calculated from equation (15) for varying initial radius (r_0) and diffusion coefficient (D). For each simulation for different r_0, Δr_0 is defined as the difference between the stepwise value r_0 and $r_{0,\text{fit}}$. ($D_{298} + \Delta D_{298}$) instead of D_{298} from Lugg (1968) is used to calculate D by equation (19), and ΔD_{298} is systematically varied to obtain different D for the simulation. Assuming that thermal equilibrium between the droplet surface and the gas very close to the surface is achieved, the temperature dependence of the gas-phase properties is evaluated using T_d and updated in every time step. Then, a simulated radius as a function of time ($r_{\text{sim}}(t)$) is calculated from the model and compared with experimental values of radius ($r_{\text{exp}}(t)$). The simulation residual, $\sum_i \left(r_{\text{sim}}(t_i) - r_{\text{exp}}(t_i)\right)^2$, is calculated and plotted as a function of (Δr_0, $\Delta D_{298}/D_{298}$). This allows the best fitted values of (Δr_0, $\Delta D_{298}/D_{298}$) to be obtained from the combination in values that has the minimum value of simulation residual. Then, r_0 and D are updated and used to simulate the evaporation profile again. The recalculated ($r_{\text{sim}} - r_{\text{exp}}$) and ($T_d - T_\infty$) as a function of time are evaluated to monitor the simulation procedure. Then, by systematic variation of α_M and V_g, a comparison between the measurement and simulation leads to a full evaluation of the simulation residuals and an identification of the best fitted values of (α_M, V_g, Δr_0, and $\Delta D_{298}/D_{298}$). An example of the dependence of the simulation residual on

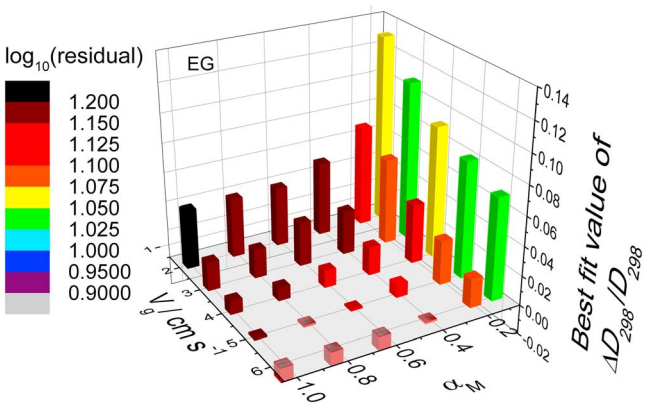

Figure 4. The best fit value of $\Delta D_{298}/D_{298}$ and simulation residual at given (α_M and V_g) from evaporation profile of EG at 20°C, 200 cm^3/min.

the three parameters (α_M, V_g, and $\Delta D_{298}/D_{298}$) is shown in Figure 4 for an EG droplet evaporation measurement.

3.4. Determination of α_M and Diffusion Coefficient

It is observed from monitoring result of the simulation procedure that the value of the Δr_0 is very close to zero and much smaller than the possible error in the size determination (±100 nm (Davies, 2014; Rovelli et al., 2016)).The relative difference of the residual across all trial combinations of fit parameters is less than 2 (equally 0.3 in log scale, as shown in Figure 4) over the range investigated, as shown in Figure 4, suggesting that the Δr_0 and residual are not sufficiently significant to be used as criteria in determination of the plausible range of α_M for EG and other organics investigated in this work. Indeed, different combinations of (α_M, V_g, and $\Delta D_{298}/D_{298}$) can essentially lead to the same time dependence in radius within the experimental uncertainty. Thus, α_M can only be determined if additional constraints can be imposed on the values of V_g and $\Delta D_{298}/D_{298}$, thereby constraining the retrieved value of α_M. V_g is only dependent on the well-controlled flow rate in the EDB, while $\Delta D_{298}/D_{298}$ is constant and assumed independent of T and V_g.

3.4.1. Evaluation of Gas Velocity Range

In previous work (Davies, 2014), the dependence of the gas flow velocity (V_g) on the gas flow rate for the same EDB has been calibrated carefully by means of force balance method. The determined V_g at 50, 100, and 200 cm^3/min are 0.8, 1.7, and 3.1 cm/s, respectively, with uncertainty of 0.8 cm/s. During evaporation kinetics measurement of single supercooled water droplets, it was confirmed that V_g at 50 cm^3/min is in the range from 0.84 cm/s (assuming $\alpha_M = 1$) to 1.47 cm/s ($\alpha_M = 0.1$) (Davies et al., 2014). Assuming linearity in the relationship of V_g to the gas flow rate, the possibility of $V_g < 1.7$ cm/s and $V_g < 3.1$ cm/s can be excluded for flow rates of 100 and 200 cm^3/min, respectively, as V_g is in the range of 0.84–1.47 cm/s for 50 cm^3/min. Therefore, V_g at 50, 100, and 200 cm^3/min in this work should lie in the range of 0.84–1.47, 1.7–2.5, and 3.1–3.9 cm/s, respectively.

3.4.2. Estimation and Evaluation of Diffusion Coefficients

Lugg (1968) and Tang et al. (2015a) have compiled and evaluated the diffusion coefficients for many organic compounds in air. However, the proposed values of uncertainty do not match well with each other. For the organic compounds of interest, the values of D_{298} estimated from the Fuller method (Tang et al., 2015b) are all higher than the experimental values from Lugg (1968) by 5–14%. The deviation, used as the uncertainty in D_{298} by Tang et al. (2015a), is also greater than the standard deviation from observations (Lugg, 1968).

In this work, the diffusion coefficients for the organics of interest at 298 K in nitrogen are estimated by using Chapman-Enskog kinetic theory (Bird et al., 2002). An evaluation of the calculated values of D_{298} from different methods, including Wilke-Lee, Fuller and Chapman-Enskog (Erbil & Dogan, 2000; Lugg, 1968; Tang et al., 2015a), and this work is shown in Table 2.

The average of the calculated values of diffusion coefficient for the organics of interest at 298 K agrees with the experimental values (Lugg, 1968) within the expected accuracy of the method of Chapman-Enskog theory (8% (Bird et al., 2002)), as shown in Table 2. The slight difference between the calculated values for 1-butanol from different studies even using the same method is likely attributed to the difference in properties used. For example, the average values of the calculated values of diffusion coefficients for 1-butanol, EG, and DEG at 298 K are 8.64×10^{-6}, 1.02×10^{-5}, and 7.53×10^{-6} m^2/s with relative standard deviation (RSD) of 4.5%, 10.1%, and 8.7%, respectively, as shown in Table 2. The relative deviations of these average values with respect to the experimental values are 0.39%, 0.84%, and 3.2%, which are much smaller than the RSD of the average values. This suggests that the experimental values from Lugg (1968) are accurate.

Using the RSD value of D_{298} from Lugg (1968) (referred to as $u(D_{298})/D_{298}$), a range on $\Delta D_{298}/D_{298}$ is used as a constraint to determine the plausible range of α_M for 1-butanol, EG, and DEG. For glycerol, the calculated D_{298} obtained in this work is 7.63×10^{-6} m^2/s. As no experimental value has been reported, the claimed accuracy of the method is ~8% (Bird et al., 2002) and will be improved later.

Table 2
Evaluation of Diffusion Coefficient for 1-Butanol, EG, DEG, and Glycerol at 298 K

	Diffusion coefficient at 298 K/m^2 s^{-1}						
	Calculated values						
Compounds	Wilke- Lee	Chen- Othmer	Fuller	Chapman-Enskog	Average of calculated values	Experimental values (Lugg, 1968)	R.D.[a]
1-butanol	8.47×10^{-6} (Lugg, 1968) 8.96×10^{-6}[b] (Erbil & Dogan, 2000)	8.53×10^{-6} (Lugg, 1968)	9.08×10^{-6} (Tang et al., 2015b) 9.07×10^{-6}[b] (Erbil & Dogan, 2000)	8.15×10^{-6} (this work) 8.24×10^{-6}[b] (Erbil & Dogan, 2000)	8.64×10^{-6} (RSD = 4.5%)	8.61×10^{-6} (RSD = 1.1%)	0.39%
EG	9.95×10^{-6} (Lugg, 1968)		1.13×10^{-5} (Tang et al., 2015b)	9.29×10^{-6} (this work)	1.02×10^{-5} (RSD = 10.1%)	1.01×10^{-5} (RSD = 3.8%)	0.84%
DEG	7.13×10^{-6} (Lugg, 1968)		8.29×10^{-6} (Tang et al., 2015b)	7.13×10^{-6} (this work)	7.53×10^{-6} (RSD = 8.7%)	7.30×10^{-6} (RSD = 1.0%)	3.2%

[a]Relative deviation of the average value of calculated value with respect to the experimental value. [b]After temperature correction from 293 K to 298 K.

With constraints on the ranges of V_g and the RSD value of literature value of diffusion coefficient at 298 K ($u(D_{298})/D_{298}$) now established, it is possible to determine the plausible range of α_M based on the combination of (α_M, V_g, and $\Delta D_{298}/D_{298}$) with the minimum residual from a comparison of predictions from the Liu model and the experimental evaporation profiles.

4. Results and Discussion

In this part, we will present the plausible ranges of α_M for EG, DEG, and 1-butanol, respectively, and then the uncertainty in the diffusion coefficient of glycerol.

4.1. Determination of α_M for EG

4.1.1. The Plausible Range of α_M for EG

Experimental data for three EG droplets evaporating at 20°C and under flow rates of 50, 100, and 200 cm^3/min are shown in Figure 3a. For convenient representation of the data analysis, the fit value of $\Delta D_{298}/D_{298}$ is reported as a function of trial values of V_g assuming that α_M = 0.1, 0.2, 0.4, and 1. These results are shown in Figure 5. For the three repeated experiments, the standard deviations of $\Delta D_{298}/D_{298}$ at each trial value of V_g are better than 0.006 and are plotted as error bars.

As described in section 3.4.1, V_g at 50, 100, and 200 cm^3/min should lie in the range of 0.84–1.47, 1.7–2.5, and 3.1–3.9 cm/s, respectively. As discussed in section 3.4.2, $\Delta D_{298}/D_{298}$ for EG should lie in the range of −0.038 and 0.038 taking the proposed RSD value of D_{298} ($u(D_{298})/D_{298}$) from Lugg (1968). The plausible ranges of (V_g and $\Delta D_{298}/D_{298}$) at 50, 100, and 200 cm^3/min are indicated in Figure 5. When α_M equals 0.1 and 0.2, the curves obtained from fitting of experimental data do not all simultaneously intersect with the allowed ranges in $\Delta D_{298}/D_{298}$, indicated by the corresponding rectangle regions, as shown in Figures 5a and 5b. Therefore, $\alpha_M < 0.2$ can be easily excluded for EG.

4.1.2. Effect of Accuracy of the Vapor Pressure

The parameterization of vapor pressure (p_v) of EG from Yaws (1994) is used in this study to calculate p_v at 298 K (7.45 Pa). Furthermore, the parameterizations and experimental vapor pressure values for EG at 20°C and 25°C reported in the literature (Ambrose & Hall, 1981; Ethylene Glycol Product Guide, 2008; Hales et al., 1981; Yaws, 1994) were evaluated. The average predicted value of p_v at 20°C is 7.50 Pa with RSD of 1.74%. The value of p_v used in this study is 0.74% greater than the experimental value (7.4 Pa) (Hales et al., 1981) and −0.56% smaller than the average value calculated above. Therefore, the RSD of p_v for EG at 20°C is set conservatively to be ±0.8% in this study. Because temperature suppressions during the evaporation process and the saturation fraction of vapor in the flowing gas (S) can be neglected, equation (14) is simplified as

$$r\frac{dr}{dt} = \frac{Sh}{2}\frac{M_v}{\rho R T_\infty} a_{solute} D p_v \beta_M \quad (20)$$

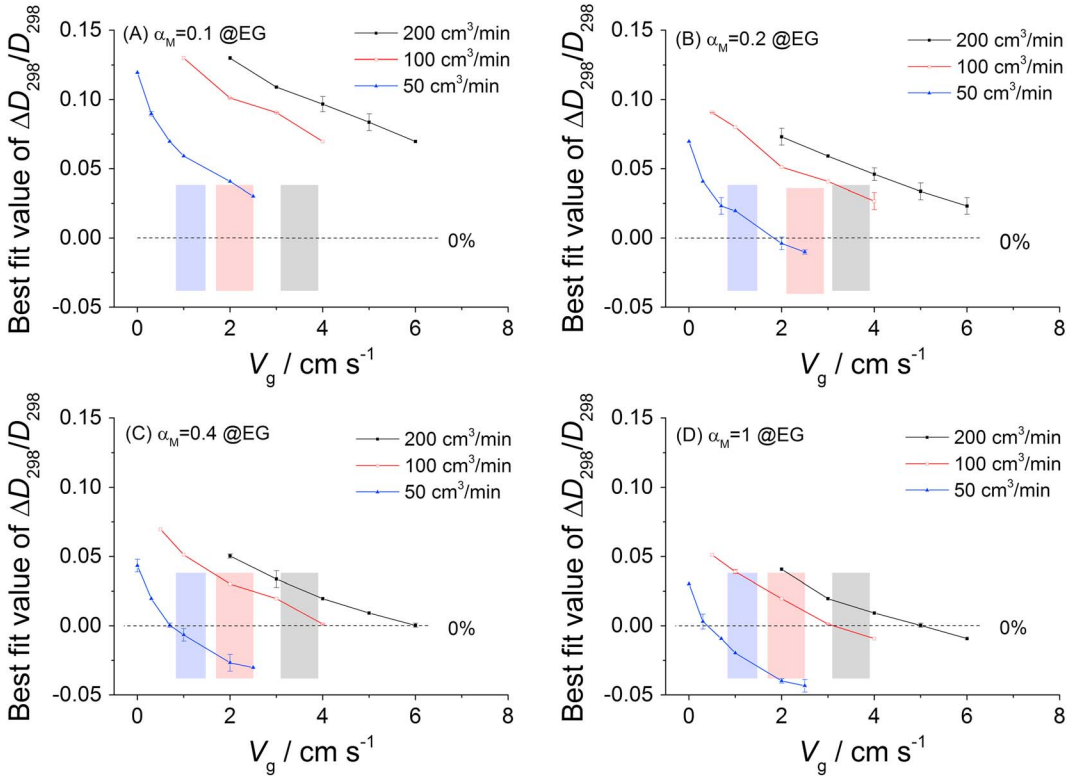

Figure 5. The best fit value of $\Delta D_{298}/D_{298}$ of EG as a function of the gas flow velocity (V_g) assuming (a) α_M = 0.1, (b) α_M = 0.2, (c) α_M = 0.4, and (d) α_M = 1 under three flow rates. The colored areas indicate the acceptable ranges for values of V_g and $\Delta D_{298}/D_{298}$ at the three flow rates (as discussed in section 3.4).

$D \times p_v$ is approximately constant as all other parameters are either constant or nearly constant. Then the possible error incurred in $\Delta D_{298}/D_{298}$ due to uncertainty in p_v is around ±0.008.

4.1.3. Refinement of α_M Range for EG

We have attempted to further constrain the best fit α_M range by taking into account the interference from moisture and the effect of impurities. In Figures 5c and 5d, the fitted V_g at 50 cm^3/min is below the expected range (marked in light blue) when the fitted V_g at the other two flow rates fall in their expected ranges. This phenomenon could perhaps arise from moisture interference from environment during EDB measurement. When the flow rate was set to be 50 cm^3/min, the gas velocity of the flow surrounding the evaporating droplet was low. Moisture from the environment could possibly penetrate through the flow, and water vapor could be absorbed by the trapped droplet. Based on the hygroscopicity of EG (EG Product Guide, 2008), the mass percent of water in the droplet at equilibrium at low RH (<25%) is below 10%. Thus, the actual a_{solute} in the measurement could be several percent lower than unity which is used in the fitting. Thus, according to equation (20), the $\Delta D_{298}/D_{298}$ presented here is underestimated by several percent. Correcting for moisture content would shift the $\Delta D_{298}/D_{298}$-V_g curve upward at 50 cm^3/min.

The possible effect of impurities introduced from reagents must also be considered. When the radius of the evaporating EG droplet decreases from 22 μm to 10 μm, the concentration of impurities in the droplet would be expected to increase from <1% to <8% based on the reported purity of EG reagent (>99%). The existence of an impurity at this content level would suppress the evaporation rate of solute, leading to an underestimate of $\Delta D_{298}/D_{298}$ in Figure 5. This would suggest that the impact of impurities would act to shift the $\Delta D_{298}/D_{298}$-V_g curves upward, suggesting that our reported lower limits on α_M should be considered very much as lower bounds on the value. Marek and Straub (2001) summarized that impurities (such as dissolved glass components, fatty acids, and surfactants) in water could cause a strong reduction in the observed evaporation coefficient of water. As the detailed composition of EG reagent is unknown, it is very challenging to estimate the effect of impurities further.

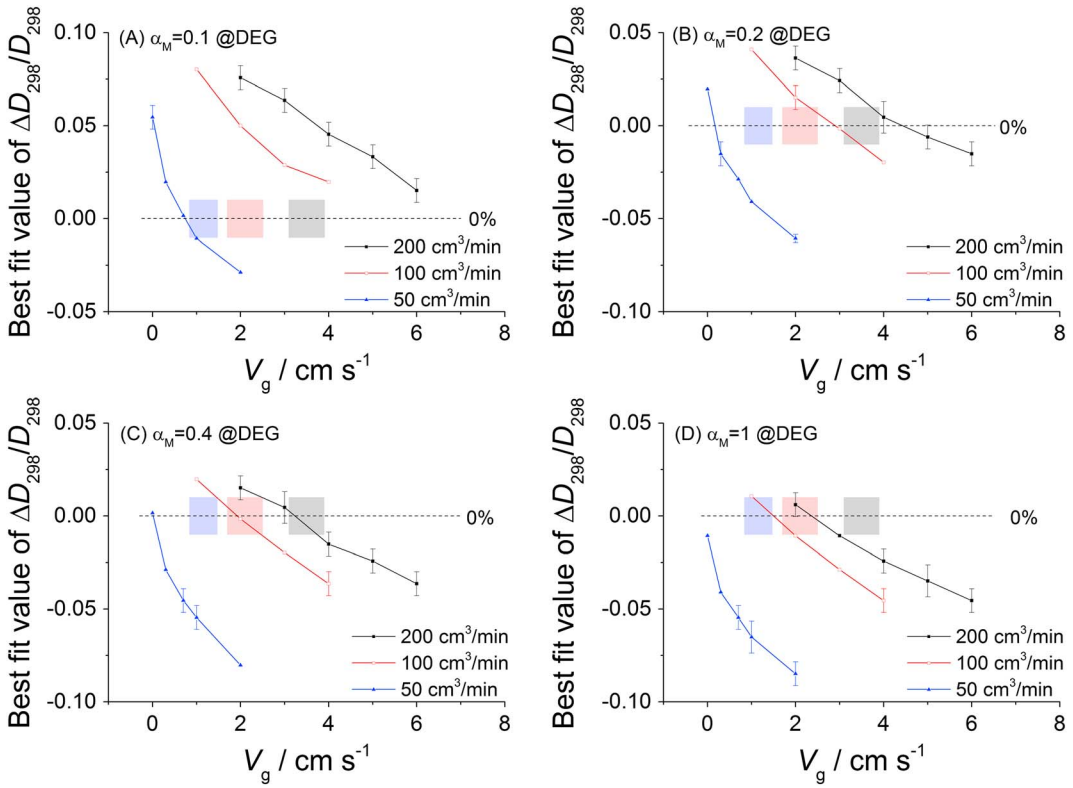

Figure 6. The best fit value of $\Delta D_{298}/D_{298}$ of DEG as a function of V_g assuming (a) $\alpha_M = 0.1$, (b) $\alpha_M = 0.2$, (c) $\alpha_M = 0.4$, and (d) $\alpha_M = 1$ under three flow rates. The colored areas indicate the acceptable ranges for values of V_g and $\Delta D_{298}/D_{298}$ at the three flow rates.

4.1.4. Summary

From Figure 5b, $\alpha_M < 0.2$ can be excluded. Taking into account the likely underestimation of $\Delta D_{298}/D_{298}$ caused by moisture interference and impurity effect, α_M should be greater than 0.4. This range is above the result from Jakubczyk et al. (2010) and agrees with the result from Tsuruta et al. (1994). Limited by the accuracies of D_{298} for EG and V_g in the EDB measurement, it is difficult to constrain the α_M range further in this study. In Figures 5c and 5d, the fitted points of (V_g and $\Delta D_{298}/D_{298}$) falling within the rectangle regions are all above the zero line ($\Delta D_{298}/D_{298} = 0$). This indicates that the true value of D_{298} might be a little higher than the present value used in this study.

4.2. Determination of α_M for DEG

DEG evaporates much more slowly than EG under the same conditions, and its evaporation rate increases with gas flow rate, as shown in Figure 3b. Experimental data from two DEG droplets were processed. $\Delta D_{298}/D_{298}$ for DEG as a function of V_g are reported in Figure 6 assuming that $\alpha_M = 0.1$, 0.2, 0.4, and 1. As described in section 3.4.1, V_g at 50, 100, and 200 cm^3/min should lie in the ranges of 0.84–1.47, 1.7–2.5, and 3.1–3.9 cm/s, respectively. As discussed in section 3.4.2, $\Delta D_{298}/D_{298}$ for DEG should lie in the range of −0.01 and 0.01 taking the proposed RSD value of experimental value of D_{298} ($u(D_{298})/D_{298}$) from Lugg (1968). The acceptable ranges of (V_g and $\Delta D_{298}/D_{298}$) at 50, 100, and 200 cm^3/min are indicated by the rectangular regions in Figure 6. When α_M equals 0.1, the curve obtained from fitting of experimental data does not cross the corresponding rectangle, as shown in Figure 6a. Thus, $\alpha_M < 0.1$ can be easily excluded.

In this work, the parameterization from DiEthylene Glycol Product Guide (2005) was used to estimate the vapor pressure (p_v) of DEG at 20°C (as shown in Table 1) and is 3% higher than the value predicted by Ambrose and Hall (1981). This would possibly introduce error in the fitted $\Delta D_{298}/D_{298}$ according to equation (20). The phenomenon caused by the moisture interference during measurement is also observed for DEG evaporating at 50 cm^3/min, as shown in Figures 6b and 6c.

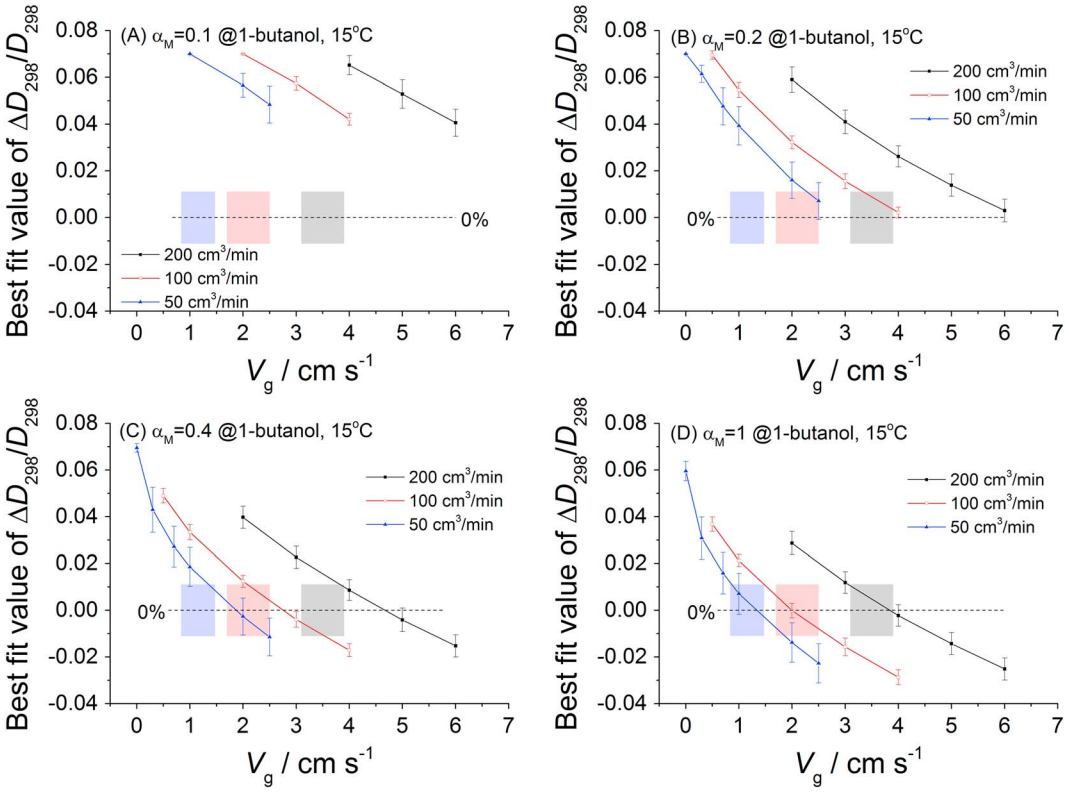

Figure 7. The best fit value of $\Delta D_{298}/D_{298}$ of 1-butanol as a function of V_g assuming (a) $\alpha_M = 0.1$, (b) $\alpha_M = 0.2$, (c) $\alpha_M = 0.4$, and (d) $\alpha_M = 1$ under three flow rates. The colored squares indicated the acceptable ranges for values of V_g at the three flow rates.

It is confirmed from Figure 6a that $\alpha_M < 0.1$ can be excluded. Taking into account the likely underestimation of $\Delta D_{298}/D_{298}$ caused by moisture interference and an impurity effect, α_M should be greater than 0.2, as shown in Figure 6b. This range is higher than previous experimental results (Jakubczyk et al., 2010) but consistent with later simulation and experimental results (Hołyst et al., 2013). If the accuracy of D_{298} and p_v for DEG could be improved, it would be possible to refine the range of α_M.

4.3. Determination of α_M for 1-Butanol

4.3.1. The Plausible Range of α_M for 1-Butanol

Experimental data of ten 1-butanol droplets beyond 1.5 s (total time of around 2.5 s) were processed, and the fitted $\Delta D_{298}/D_{298}$ as a function of trial V_g are reported in Figure 7 assuming that α_M = 0.1, 0.2, 0.4, and 1, respectively. Comparing with EG and DEG, the 1-butanol droplet evaporates much faster. Thus, the number of data points available for fitting is much less and the precision of the fitted $\Delta D_{298}/D_{298}$ for 1-butanol is worse. As described in section 3.4.1, V_g at 50, 100, and 200 cm^3/min should lie in the range of 0.84–1.47, 1.7–2.5, and 3.1–3.9 cm/s, respectively, while $\Delta D_{298}/D_{298}$ for 1-butanol should lie in the range of −0.011 and 0.011, taking the proposed RSD value of D_{298} from Lugg (1968). The acceptable ranges of (V_g and $\Delta D_{298}/D_{298}$) at 50, 100, and 200 cm^3/min are marked by the rectangle regions with colors of light blue, light red, and gray, respectively, as shown in Figure 7. Values of the mass accommodation coefficient (α_M) less than 0.2 can be easily excluded according to Figures 7a and 7b.

4.3.2. Refinement of α_M Range for 1-Butanol

The effect of temperature suppression caused by solvent evaporation, residual water or ethanol in the droplet, moisture interference in the gas phase, and impurities from reagents will be taken into account to refine α_M range for 1-butanol.

As the solvents (ethanol and water) evaporate much faster than the solute and the resulting temperature suppression is severe, the droplet may not be able to recover fully on the experimental timescale to achieve a thermal equilibrium. These suggest that the actual T_d in the measurement may be lower than the estimated

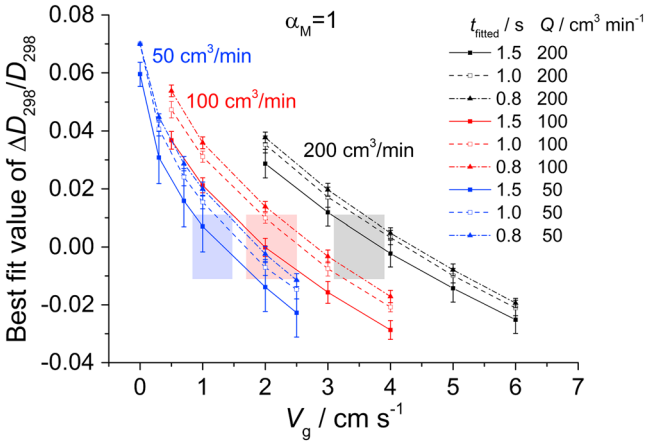

Figure 8. Effects of the data range selected for fitting on the best fit $\Delta D_{298}/D_{298}$-V_g curve at three gas flow rates assuming α_M = 1.

value from equation (15) based on the assumption of thermal equilibrium. The use of an overestimated T_d in the fitting would result in an underestimation of fitted $\Delta D_{298}/D_{298}$ to obtain the same evaporation profile.

It is difficult to determine exactly when the mole fractions of ethanol and water become very small; instead, data points beyond t_{fitted} = 0.8, 1.0, and 1.5 s were only extracted from the evaporation profiles for fitting and the outcomes were compared. The obtained $\Delta D_{298}/D_{298}$-V_g curve shifts upward as t_{fitted} decreases from 1.5 s to 0.8 s and the absolute variance is around 1% for 200 cm^3/min, as shown in Figure 8. This might be attributed to the evaporation of residual solvents in the droplet. A larger t_{fitted} was not chosen as less than 100 data points were extracted, and the precision of the fitted result became worse. The overall consequences of this comparison suggest that a value of α_M = 1 becomes more consistent with the date as earlier parts in the evaporation are excluded from the fitting.

1-butanol is hydrophobic; hence, there is a limited effect of environmental moisture at 50 cm^3/min. For the fitted points at three flow rates falling in the rectangle regions, the fitted values of $\Delta D_{298}/D_{298}$ are similar, while the corresponding V_g values fulfill the relationship with flow rates, as shown in Figures 7c and 7d. Taking into account the possible underestimation of effect of thermal nonequilibrium and impurity during measurement, the $\Delta D_{298}/D_{298}$-V_g curves should be shifted upward and α_M should be greater than 0.4, as shown in Figure 7c.

4.3.3. Effect of Accuracy of VaporPressure (p_v) and Evaluation of Literature Parameterizations

The predicted values of vapor pressure (p_v) of 1-butanol from different parameterizations (Munday et al., 1980; Schmeling & Strey, 1983; Riddick et al., 1986; Gregorowicz et al., 1987; http://ddbonline.ddbst.com/AntoineCalculation/AntoineCalculationCGI.exe; Ahn & Liu, 1990; Dean, 1992; Yaws, 1994; Liley et al. 1999; Poling et al., 2008; Yaws, 2015) are not consistent and do not match the experimental values (Butler et al., 1935; Puck & Wise, 1946; Kemme & Kreps, 1969; Ambrose & Sprake, 1970; Gracia et al., 1992; Garriga et al., 2002) well, as shown in Figure 9. As described in section 2.1.2, the parameterization from Yaws (1994) was used to estimate p_v for 1-butanol in this study. Experimental values of p_v at 298 K obtained by other researchers (marked with circles) are 4.3% and 8.5% lower than the used value. Using the parameterization from Ahn and Liu (1990), the predicted value of p_v at 298 K agrees well with the value from Haynes (2016). If this parameterization is used instead of Yaws's for fitting, the fitted $\Delta D_{298}/D_{298}$ would increase by 0.085 with respect to the value shown in Figure 7. The $\Delta D_{298}/D_{298}$-V_g curves would be shifted upward by 0.085 and beyond the rectangle region even when α_M equals unity. This indicates that the value of p_v at 298 K from Haynes (2016) might be lower than the true value.

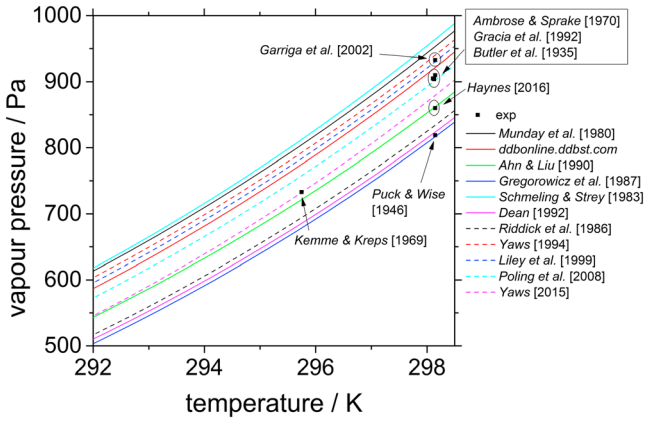

Figure 9. Experimental values (points) and parameterizations (lines) of vapor pressure as a function of temperature for 1-butanol available in the literature.

4.3.4. Summary

It is confirmed that $\alpha_M < 0.2$ can be excluded. Taking into account the possible underestimation of fitted $\Delta D_{298}/D_{298}$ caused by thermal nonequilibrium and impurity during measurement, α_M should be greater than 0.4. The proposed value of p_v at 298 K from Haynes (2016) might be lower by several percent.

4.4. Determination of Diffusion Coefficient for Glycerol

As the reported values of α_M for glycerol are greater than 0.34 (McFeely & Somorja, 1972) and even larger (Cammenga et al., 1977; Lednovich & Fenn, 1977), sensitivity analysis shows that the evaporation kinetics should be more sensitive to the diffusion coefficient than to α_M. Therefore, measurements under only the commonly used condition of EDB (20°C, 200 cm^3/min) were performed. Experimental data for two glycerol droplets were processed, and the 2-D contour of $\Delta D_{298}/D_{298}$ as a function of (α_M and V_g) is reported in Figure 10. The fitting of

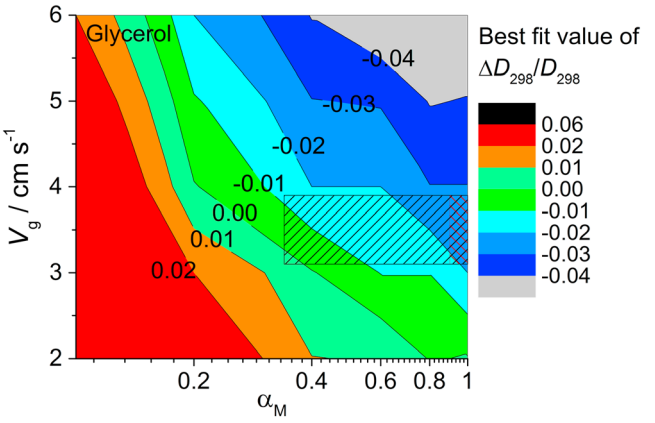

Figure 10. Two-dimensional contour of the best fit value of $\Delta D_{298}/D_{298}$ as a function of (α_M and V_g) from evaporation profile of glycerol at 20°C, 200 cm^3/min. The shaded box represents the acceptable area of (α_M and V_g) from literatures ($\alpha_M > 0.34$ in black and $\alpha_M > 0.90$ in red) and are used to improve the accuracy of diffusion coefficient for glycerol.

data of two glycerol droplets show that the standard deviation of fitted $\Delta D_{298}/D_{298}$ at given (α_M andV_g) is less than 0.007. The parameterization of vapor pressure for glycerol from Cammenga et al. (1977) was used in this study and compared with that from Coker (2010). The relative difference between the predicted values of p_v at 20°C from the two parameterizations is 0.73%, comparable with the absolute accuracy claimed in Cammenga et al. (1977).

As discussed before, V_g at 200 cm^3/min should lie in the range of 3.1–3.9 cm/s. When α_M greater than 0.34 (McFeely & Somorja, 1972) is used as a constraint, the possible range of (α_M and V_g) is marked by the black shaded box, as shown in Figure 10. The likely range of fitted $\Delta D_{298}/D_{298}$ is between −3% and 1%. If α_M is constrained to have a value greater than 0.9 (Lednovich & Fenn, 1977), the possible range of (α_M and V_g) is marked by the red rectangle with oblique line. The likely range of fitted $\Delta D_{298}/D_{298}$ is between −3% and −1%. We conclude that the RSD of D_{298} should lie in the range of −3% and −1%, which is much better than the expected accuracy of the method from Chapman-Enskog theory (8 % (Bird et al., 2002)).

5. Conclusions

In order to accurately quantify the kinetics of mass transfer between the gas and condensed phases in aerosol, physicochemical properties of the gas and condensed phases as well as kinetic parameters are crucial for estimating mass fluxes over a wide size range. Comparing with physicochemical properties, the kinetic parameters such as mass accommodation coefficient/evaporation coefficient remain to be accurately determined. In this work, we aim to clarify the discrepancies in the reported values of evaporation coefficient (α_M) for 1-butanol, ethylene glycol (EG), and diethylene glycol (DEG) and improve the accuracy of diffusion coefficient for glycerol.

Simulations based on Liu model (Ahn & Liu, 1990) have been used to describe the heat and mass transfer at the evaporating droplet surface. We have first verified this model by comparing predictions for the evaporation of pure water droplets with measurements using the cylindrical electrode electrodynamic balance (EDB), along with a comparison with predictions from the Kulmala model (Kulmala et al., 1993). This demonstrates that Liu model is sufficiently accurate to describe the evaporation/condensation kinetics of compounds investigated in this work. The sensitivity of evaporation kinetics to the value of α_M for 1-butanol has been evaluated using this approach. The evaporation rate increases with α_M, and the experimental error envelop overlaps with simulations when α_M is greater than 0.6, suggesting that this is an upper limit for determination using the EDB approach if all other quantities are known exactly. Clearly, uncertainties in the other physicochemical parameters further lower the accessible limit below which values of α_M can be directly determined.

We report evaporation profiles of 1-butanol, EG, DEG, and glycerol droplets under well-determined conditions (gas flow rates and temperature) using the EDB technique with a time resolution of 10 ms. For single-component organic droplets, the time-resolved radius recorded from experiments is fitted using Liu model with varying experimental conditions (e.g., gas velocity, V_g) and differing treatments of the key thermophysical properties (the evaporation coefficient, α_M, the diffusion coefficient at 298 K). The fitted values of (α_M, V_g, and $\Delta D_{298}/D_{298}$) corresponding to the best agreement between model prediction and experimental data are obtained.

The uncertainties in the thermophysical and possible errors in experimental conditions were carefully evaluated. The calculated values of D_{298} from different methods, including Wilke-Lee, Fuller, and Chapman-Enskog, in the literature and this work were evaluated and compared with experimental values. This comparison demonstrates that the experimental values from Lugg (1968) are accurate. The gas velocities (V_g) at three gas flow rates were evaluated based on previous studies, and the plausible ranges were obtained. With these constraints on the accuracy of D_{298} and V_g, the impossible range of α_M could be easily excluded. The possible error in experimental conditions, such as moisture interference and impurities effect, was taken into account to refine the range of α_M further.

Results show that α_M should be greater than 0.4 for EG. This range is beyond the result from Jakubczyk et al. (2010) and agrees with the result from Tsuruta et al. (1994). The fitted points of (V_g and $\Delta D_{298}/D_{298}$) falling within the rectangle regions are all above the zero line ($\Delta D_{298}/D_{298} = 0$), which indicates that the true value of D_{298} might be a little higher than the present value used in this study. For DEG, α_M should be greater than 0.2. This range is higher than previous experimental results (Jakubczyk et al., 2010) but consistent with their later simulation and experimental results (Hołyst et al., 2013). For 1-butanol, α_M should be greater than 0.4, while the proposed value of vapor pressure at 298 K from CRC handbook might be lower by several percent. For glycerol, the likely range of fitted $\Delta D_{298}/D_{298}$ is between −3% and 1% when α_M greater than 0.34 (McFeely & Somorja, 1972) is used as a constraint. If α_M is constrained to have a value greater than 0.9 (Lednovich & Fenn, 1977), the likely range of fitted $\Delta D_{298}/D_{298}$ is between −3% and −1%. Therefore, the accuracy of D_{298} is much improved comparing with the expected accuracy of the method from Chapman-Ensokog theory (8%) (Bird et al., 2002).

Acknowledgments

Y. S. S. acknowledges financial support from the National Key Foundation for Exploring Scientific Instrument of MOST of China (2012YQ250003). J. P. R. acknowledges the Natural Environment Research Council (grant NE/L006901/1) for funding. A. M. thanks EPSRC for DTA.The authors comply with AGU's data policy and declare no competing financial interest. The data used are listed at https://doi.org/10.5523/bris.130ygtby4qslw2w8o6uzkpyo9x.

References

Agarwal, J. K., & Sem, G. J. (1980). Continuous flow, single-particle-counting condensation nucleus counter. *Journal of Aerosol Science*, *11*(4), 343–357. https://doi.org/10.1016/0021-8502(80)90042-7

Ahn, K. H., & Liu, B. Y. H. (1990). Particle activation and droplet growth process in condensation nucleus counter—I. Theoretical background. *Journal of Aerosol Science*, *21*(2), 249–261. https://doi.org/10.1016/0021-8502(90)90008-L

Ambrose, D., & Hall, D. J. (1981). Thermodynamic properties of organic oxygen compounds L:The vapour pressures of 1, 2-ethanediol (ethylene glycol) and bis (2-hydroxyethyl) ether (diethylene glycol). *The Journal of Chemical Thermodynamics*, *13*(1), 61–66. https://doi.org/10.1016/S0021-9614(81)80009-2

Ambrose, D., & Sprake, C. H. S. (1970). Thermodynamic properties of organic oxygen compounds. XXV. Vapour pressures and normal boiling temperatures of aliphatic alcohols. *Journal of Chemical Thermodynamics*, *2*, 631–645. https://doi.org/10.1016/0021-9614(70)90038-8

Bird, R. B., Stewart, W. E., & Lightfoot, E. N. (Eds.) (2002). *Transport Phenomenon* (2nd ed.). New York: John Wiley.

Butler, J. A. V., Ramchandani, C. N., & Thomson, D. W. (1935). The solubility of nonelectrolytes. Part I. The free energy of hydration of some aliphatic alcohols. *Journal of the Chemical Society*, 280–285. https://doi.org/10.1039/JR9350000280

Cammenga, H. K., Schulze, F. W., & Theuerl, W. (1977). Vapor pressure and evaporation coefficient of glycerol. *Journal of Chemical & Engineering Data*, *22*(2), 131–134. https://doi.org/10.1021/JE60073a004

Coker, A. K. (2010). *Ludwig's applied process design for chemical and petrochemical plants* (Vol. 2, 4th ed.), Appendix C. Oxford, UK: Elsevier/Gulf Professional.

Davies, J. F. (2014).Characterising the impact of bulk, surface and gas-phase limitations on mass transport in aerosol, Phd dissertation, University of Bristol.

Davies, J. F., Haddrell, A. E., & Reid, J. P. (2012). Time-resolved measurements of the evaporation of volatile components from single aerosol droplets. *Aerosol Science and Technology*, *46*(6), 666–677. https://doi.org/10.1080/02786826.2011.652750

Davies, J. F., Haddrell, A. E., Rickards, A. M. J., & Reid, J. P. (2013). Simultaneous analysis of the equilibrium hygroscopicity and water transport kinetics of liquid aerosol. *Analytical Chemistry*, *85*(12), 5819–5826. https://doi.org/10.1021/ac4005502

Davies, J. F., Miles, R. E. H., Haddrell, A. E., & Reid, J. P. (2014). Temperature dependence of the vapor pressure and evaporation coefficient of supercooled water. *Journal of Geophysical Research: Atmospheres*, *119*, 10,931–10,940. https://doi.org/10.1002/2014JD022093

Dean, J. A. (Ed.) (1999). *Lange's Handbook of Chemistry (15th)*. New York: McGraw-Hill.

Dean, J. D. (Ed.) (1992). *Lange's Handbook of Chemistry (14th)*. New York: McGraw-Hill.

Devarakonda, V., & Ray, A. K. (2000). Determination of thermodynamic parameters from evaporation of binary microdroplets of volatile constituents. *Journal of Colloid and Interface Science*, *221*(1), 104–113. https://doi.org/10.1006/jcis.1999.6580

DiEthylene Glycol Product Guide (2005). The MEGlobal Group of Companies.

Erbil, H. Y., & Dogan, M. (2000). Determination of diffusion coefficient-vapor pressure product of some liquids from hanging drop evaporation. *Langmuir*, *16*(24), 9267–9273. https://doi.org/10.1021/la000721b

Ethylene Glycol Product Guide (2008). The MEGlobal Group of Companies.

Fuchs, N. A. (1959). *Evaporation and droplet growth in gaseous media*. Oxford: Pegamon.

Garriga, R., Martinez, S., Pérez, P., & Gracia, M. (2002). Vapor pressures at several temperatures between 278.15 and 323.15 K and excess functions at T = 298.15 K for 1-Bromobutane with 1-Butanol or 2-Methyl-2-propanol. *Journal of Chemical & Engineering Data*, *47*(2), 322–328. https://doi.org/10.1021/je0101754

Giechaskiel, B., Wang, X., Gillil, D., & Drossinos, Y. (2011). The effect of particle chemical composition on the activation probability in n-butanol condensation particle counters. *Journal of Aerosol Science*, *42*(1), 20–37. https://doi.org/10.1016/j.jaerosci.2010.10.006

Gracia, M., Sanche, F., Prerez, P., Valero, J., & Cuterrez Losa, C. (1992). Vapour pressures of (butan-1-ol + hexane) at temperatures between 283.10 K and 323.12 K. *Journal of Chemical Thermodynamics*, *24*, 463–471. https://doi.org/10.1016/S0021-9614(05)80118-1

Gregorowicz, J., Kiciak, K., & Malanowsk, S. (1987). Vapour pressure data for 1-butanol, cumene, n-octane and n-decane and their statistically consistent reduction with the antoine equation. *Fluid Phase Equilihrta*, *38*(1-2), 97–107. https://doi.org/10.1016/0378-3812(87)90006-9

Hales, J. L., Cogman, R. C., & Frith, W. J. (1981). A transpiration-g.l.c. apparatus for measurement of low vapour concentration. *The Journal of Chemical Thermodynamics*, *13*(6), 591–601. https://doi.org/10.1016/0021-9614(81)90117-8

Haynes, W. M. (Ed.) (2016). *CRC Handbook of Chemistry and Physics (96th Edition, Internet Version)*. Boca Raton, FL: CRC Press/Taylor and Francis.

Hering, S. V., & Stolzenburg, M. R. (2005). A method for particle size amplification by water condensation in a laminar, thermally diffusive flow. *Aerosol Science and Technology*, *39*(5), 428–436. https://doi.org/10.1080/027868290953416

Hinds, W. C. (1999). *Aerosol Technology: Properties, Behavior, and Measurement of Airborne Particles* (2nd ed.). New York: John Wiley.

Hołyst, R., Litniewski, M., Jakubczyk, D., Zientara, M., & Wózniak, M. (2013). Nanoscale transport of energy and mass flux during evaporation of liquid droplets into inert gas: Computer simulations and experiments. *Soft Matter*, *9*(32), 7766–7774. https://doi.org/10.1039/c3sm50997d

Hopkins, R. J., & Reid, J. P. (2005). Evaporation of ethanol/water droplets: Examining the temporal evolution of droplet size, composition and temperature. *The Journal of Physical Chemistry. A*, *109*(35), 7923–7931. https://doi.org/10.1021/jp0516543

Iida, K., Stolzenburg, M. R., & McMurry, P. H. (2009). Effect of working fluid on sub-2 nm particle detection with a laminar flow ultrafine condensation particle counter. *Aerosol Science and Technology*, *43*(1), 81–96. https://doi.org/10.1080/02786820802488194

Jakubczyk, D., Derkachov, G., Duc, T. D., Kolwas, K., & Kolwas, M. (2010). Coefficients of evaporation and gas phase diffusion of low-volatility organic solvents in nitrogen from interferometric study of evaporating droplets. *The Journal of Physical Chemistry. A*, *114*(10), 3483–3488. https://doi.org/10.1021/jp911466e

Kangasluoma, J., Franchin, A., Duplissy, J., Ahonen, L., Korhonen, F., Attoui, M., … Petäjä, T. (2015). Operation of the Airmodus A11 nano condensation nucleus counter at various inlet pressures, various operation temperatures and design of a new inlet system. *Atmospheric Measurement Techniques Discussions*, *8*(8), 8483–8508. https://doi.org/10.5194/amtd-8-8483-2015

Kangasluoma, J., Kuang, C., Wimmer, D., Rissanen, M. P., Lehtipalo, K., Ehn, M., … Petäjä, T. (2014). Sub-3 nm particle size and composition dependent response of a nano-CPC battery. *Atmospheric Measurement Techniques*, *7*(3), 689–700. https://doi.org/10.5194/amt-7-689-2014

Kemme, H. R., & Kreps, S. I. (1969). Vapor pressure of primary n-alkyl chlorides and alcohols. *Journal of Chemical Engineering Data*, *14*(1), 98–102. https://doi.org/10.1021/je60040a011

Kolb, C. E., Cox, R. A., Abbatt, J. P. D., Ammann, M., Davis, E. J., Donaldson, D. J., … O'Dowd, C. D. (2010). An overview of current issues in the uptake of atmospheric trace gases by aerosols and clouds. *Atmospheric Chemistry and Physics*, *10*(21), 10,561–10,605. https://doi.org/10.5194/acp-10-10561-2010

Krieger, U. K., Marcolli, C., & Reid, J. P. (2012). Exploring the complexity of aerosol particle properties and processes using single particle techniques. *Chemical Society Reviews*, *41*(19), 6631–6662. https://doi.org/10.1039/c2cs35082c

Kulmala, M., Mordas, G., Petäjä, T., Grönholm, T., Aalto, P. P., Vehkamäki, H., … Wagner, P. E. (2007). The condensation particle counter battery (CPCB): A new tool to investigate the activation properties of nanoparticles. *Journal of Aerosol Science*, *38*(3), 289–304. https://doi.org/10.1016/j.jaerosci.2006.11.008

Kulmala, M., Vesala, T., & Wagner, P. E. (1993). An analytical expression for the rate of binary condensational particle growth. *Proceedings of the Royal Society of London A*, *441*(1913), 589–605. https://doi.org/10.1098/rspa.1993.0081

Langridge, J. M., Richardson, M. S., Lack, D. A., & Murphy, D. M. (2016). Experimental evidence supporting the insensitivity of cloud droplet formation to the mass accommodation coefficient for condensation of water vapor to liquid water. *Geophysical Research Letters*, *43*(12), 6650–6656. https://doi.org/10.1002/2016GL069328

Lednovich, S. L., & Fenn, J. B. (1977). Absolute evaporation rates for some polar and nonpolar liquids. *AIChE Journal*, *23*(4), 454–459. https://doi.org/10.1002/aic.690230408

Lemmon, E. W., & Jacobsen, R. T. (2004). Viscosity and thermal conductivity equations for nitrogen, oxygen, argon, and air. *International Journal of Thermophysics*, *25*(1), 21–69. https://doi.org/10.1023/B:IJOT.0000022327.04529.f3

Liley, P. E., Thomson, G. H., Friend, D. G., Daubert, T. E., & Buck, E. (1999). *Perry's Chemical Engineers' Handbook Section 2: Physical and Chemical Data*. New York: the McGraw-Hill Professional.

Lugg, G. A. (1968). Diffusion coefficients of some organic and other vapors in air. *Analytical Chemistry*, *40*(7), 1072–1077. https://doi.org/10.1021/ac60263a006

Marek, R., & Straub, J. (2001). Analysis of the evaporation coefficient and the condensation of water. *International Journal of Heat and Mass Transfer*, *44*(1), 39–53. https://doi.org/10.1016/S0017-9310(00)00086-7

McFeely, F. R., & Somorja, G. A. (1972). Studies of the vaporization kinetics of hydrogen-bonded liquids. *The Journal of Physical Chemistry*, *76*(6), 914–918. https://doi.org/10.1021/j100650a022

McMurry, P. H. (2000). The history of condensation nucleus counters. *Aerosol Science and Technology*, *33*(4), 297–322. https://doi.org/10.1080/02786820050121512

Miles, R. E. H., Reid, J. P., & Riipinen, I. (2012). Comparison of approaches for measuring the mass accommodation coefficient for the condensation of water and sensitivities to uncertainties in thermophysical properties. *The Journal of Physical Chemistry. A*, *116*(44), 10,810–10,825, https://doi.org/10.1021/jp3083858.

Munday, E. B., Mullins, J. C., & Edie, D. D. (1980). Vapor pressure data for toluene, I-Pentanol, I-Butanol, water, and 1-propanol and for the water and I-propanol system from 273.15 to 323.15 K. *Journal of Chemical & Engineering Data*, *25*(3), 191–194. https://doi.org/10.1021/je60086a006

Murphy, D. M., & Koop, T. (2005). Review of the vapour pressures of ice and supercooled water for atmospheric applications. *Quarterly Journal of the Royal Meteorological Society*, *131*(608), 1539–1565. https://doi.org/10.1256/qj.04.94

Persad, A. H., & Ward, C. A. (2016). Expression for the evaporation and condensation coefficients in the Hertz-Knudsen relation. *Chemical Reviews*, *116*(14), 7727–7767. https://doi.org/10.1021/acs.chemrev.5b00511

Poling, B. E., Thomson, G. H., Friend, D. G., Rowley, R. L., & Wilding, W. V. (2008). *Perry's Chemical Engineers' Handbook (8nd Edition), Section 2 Physical and Chemical Data*. New York: the McGraw-Hill Companies.

Puck, T. T., & Wise, H. (1946). Studies in vapor-liquid equilibria. I. A new dynamic method for the determination of vapor pressures of liquids. *Journal of Physical Chemistry*, *50*, 329–339. https://doi.org/10.1021/j150448a004

Raatikainen, T., Moore, R. H., Lathem, T. L., & Nenes, A. (2012). A coupled observation- modeling approach for studying activation kinetics from measurements of CCN activity. *Atmospheric Chemistry and Physics*, *12*(9), 4227–4243. https://doi.org/10.5194/acp-12-4227-2012

Reid, J. P., Dennis-Smither, B. J., Kwamena, N. A., Miles, R. E. H., Hanford, K. L., & Homer, C. J. (2011). The morphology of aerosol particles consisting of hydrophobic and hydrophilic phases: Hydrocarbons, alcohols and fatty acids as the hydrophobic component. *Physical Chemistry Chemical Physics*, *13*(34), 15,559–15,572. https://doi.org/10.1039/c1cp21510h

Riddick, J., Bunger, W. B., & Sakano, T. K. (1986). *Organic Solvents: Physical Properties and Method of Purification* (4th ed.). New York: John Wiley.

Riipinen, I., Pierce, J. R., Yli-Juuti, T., Nieminen, T., Häkkinen, S., Ehn, M., … Kulmala, M. (2011). Organic condensation: A vital link connecting aerosol formation to cloud condensation nuclei (CCN) concentrations. *Atmospheric Chemistry and Physics*, *11*(8), 3865–3878. https://doi.org/10.5194/acp-11-3865-2011

Riipinen, I., Yli-Juuti, T., Pierce, J. R., Petäjä, T., Worsnop, D. R., Kulmala, M., & Donahue, N. M. (2012). The contribution of organics to atmospheric nanoparticle growth. *Nature Geoscience*, *5*(7), 453–458. https://doi.org/10.1038/ngeo1499

Rovelli, G., Miles, R. E. H., Reid, J. P., & Clegg, S. L. (2016). Accurate measurements of aerosol hygroscopic growth over a wide range in relative humidity. *The Journal of Physical Chemistry. A*, *120*(25), 4376–4388. https://doi.org/10.1021/acs.jpca.6b04194

Saros, M. T., Weber, R. J., Marti, J. J., & McMurry, P. H. (1996). Ultrafine aerosol measurement using a condensation nucleus counter with pulse height analysis. *Aerosol Science and Technology*, *25*(2), 200–213. https://doi.org/10.1080/02786829608965391

Schmeling, T., & Strey, R. (1983). Equilibrium vapor pressure measurements for the n-alcohols in the temperature range from −30°C to +30°C. *Berichte der Bunsengesellschaft für Physikalische Chemie*, *87*(10), 871–874. https://doi.org/10.1002/bbpc.19830871008

Seinfeld, J. H., & Pandis, S. N. (2006). *Atmospheric Chemistry and Physics: From Air Pollution and Climate Change* (2nd ed.). NJ: John Wiley.

Tang, M. J., Shiraiwa, M., Pöschl, U., Cox, R. A., & Kalberer, M. (2015a). Compilation and evaluation of gas phase diffusion coefficients of reactive trace gases in the atmosphere: Volume 2. Diffusivities of organic compounds, pressure-normalised mean free paths, and average Knudsen numbers for gas uptake calculations. *Atmospheric Chemistry and Physics*, *15*(10), 5585–5598. https://doi.org/10.5194/acp-15-5585-2015

Tang, M. J., Shiraiwa, M., Pöschl, U., Cox, R. A., & Kalberer, M. (2015b). Supplement of compilation and evaluation of gas phase diffusion coefficients of reactive trace gases in the atmosphere: Volume 2. Diffusivities of organic compounds, pressure-normalised mean free paths, and average Knudsen numbers for gas uptake calculations. *Supplement of AtmosphericChemistry and Physics*, *15*, 5585–5598. https://doi.org/10.5194/acp-15-5585-2015-supplement

Topping, D., Connolly, P., & McFiggans, G. (2013). Cloud droplet number enhanced by co-condensation of organic vapours. *Nature Geoscience*, *6*(6), 443–446. https://doi.org/10.1038/ngeo1809

Tröstl, J., Chuang, W. K., Gordon, H., Heinritzi, M., Yan, C., Molteni, U., … Baltensperger, U. (2016). The role of low-volatility organic compounds in initial particle growth in the atmosphere. *Nature*, *533*(7604), 527–531. https://doi.org/10.1038/nature18271

Tsuruta, T., Kato, Y., Yasunobu, T., & Masuoka, T. (1994). Estimation of condensation coefficient by dropwise condensation method (condensation coefficients of ethylene glycol and water). *The Japan Society of Mechanical Engineers*, *60*(570), 158–164.

Tuch, T., Weinhold, K., Merkel, M., Nowak, A., Klein, T., Quincey, P., … Wiedensohler, A. (2016). Dependence of CPC cut-off diameter on particle morphology and other factors. *Aerosol Science and Technology*, *50*(4), 331–338. https://doi.org/10.1080/02786826.2016.1152351

Vehkamäki, H., & Riipinen, I. (2012). Thermodynamics and kinetics of atmospheric aerosol particle formation and growth. *Chemical Society Reviews*, *41*(15), 5160–5173. https://doi.org/10.1039/c2cs00002d

Wagner, P. E. (1982). In W. H. Marlow (Ed.), *Aerosol Microphysics. II: Chemical Physics of Microparticles* (Vol. 29, p. 129). Berlin: Springer. https://doi.org/10.1007/978-3-642-81805-9_5

Wiedensohlet, A., Orsini, D., Covert, D. S., Coffmann, D., Cantrell, W., Havlicek, M., … Litchy, M. (1997). Intercomparison study of the size-dependent counting efficiency of 26 condensation particle counters. *Aerosol Science and Technology*, *27*(2), 224–242. https://doi.org/10.1080/02786829708965469

Winkler, P. M., Vrtala, A., Rudolf, R., Wagner, P. E., Riipinen, I., Vesala, T., … Kulmala, M. (2006). Condensation of water vapor: Experimental determination of mass and thermal accommodation coefficients. *Journal of Geophysical Research*, *111*, D19202. https://doi.org/10.1029/2006JD007194

Winkler, P. M., Vrtala, A., Wagner, P. E., Kulmala, M., Lehtinen, K. E. J., & Vesala, T. (2004). Mass and thermal accommodation during gas-liquid condensation of water. *Physical Review Letters*, *93*(7), 075701-1-075701-4. https://doi.org/10.1103/PhysRevLett.93.075701

Yaws, C. L. (1994). *Handbook of Vapor Pressure* (Vol. 1 C1 to C4 Compounds, Vol. 2. C5 to C7 Compounds, Vol. 3, C8 to C28 Compounds). Houston, TX: Gulf Publishing Co.

Yaws, C. L. (2015). *The Yaws Handbook of Vapor Pressure* (2nd ed.- Antoine coefficients ed.). Amsterdam: Gulf Professional.

Zhang, Z. Q., & Liu, B. Y. H. (1990). Dependence of the performance of TSI 3020 condensation nucleus counter on pressure, flow rate, and temperature. *Aerosol Science and Technology*, *13*(4), 493–504. https://doi.org/10.1080/02786829008959464

Zientara, M., Jakubczyk, D., Kolwas, K., & Kolwas, M. (2008). Temperature dependence of the evaporation coefficient of water in air and nitrogen under atmospheric pressure: Study in water droplets. *The Journal of Physical Chemistry. A*, *112*(23), 5152–5158. https://doi.org/10.1021/jp7114324